NANO LETTERS

2007
Vol. 7, No. 11
3324−3328

Temperature-Driven Pumping of Fluid through Single-Walled Carbon Nanotubes

M. J. Longhurst and N. Quirke*

Department of Chemistry, Imperial College of Science, Technology and Medicine, South Kensington, SW7 2AY, United Kingdom

Received June 27, 2007

ABSTRACT

We describe a methodology for the continuous pumping of fluid, in this case decane, through carbon nanotubes. Fluid is imbibed from a reservoir at 300 K, heated, and subsequently ejected from the hot end. Very high pressures are developed in the smaller nanotubes due to strong capillary forces, suggesting their use as dynamic nanoscale reaction vessels. A theoretic framework is developed allowing us to predict pumping fluxes over a range of nanotube diameters and temperatures.

Since their identification in 1991,[1] carbon nanotubes (CNTs) have drawn much attention, not only for their exceptional mechanical and electrical properties, but also in the ever expanding area of nanofluidics.[2] Theoretical and empirical evidence suggest that water can enter extremely small (sub-2-nanometer) CNTs,[3,4] while theoretical studies in our group have predicted ultrafast imbibition of hydrocarbons in to these essentially frictionless pipes.[5] Possible applications are numerous, including the use of nanotubes as molecular sensors, nanopipettes, fluid filtration devices, and targeted drug delivery devices.[6−8] Because of their exceptional mechanical and thermal stability,[9] nanotubes are also ideal candidates as cavities for chemical reactions at high temperatures and pressures, or where confinement itself may open new reaction pathways.[10] Here we consider a methodology for fluid ejection, or continuous pumping of fluid through CNTs into a low-density medium. Because of their small dimensions and the nature of the intermolecular forces present, pressures develop inside CNTs that are greatly magnified compared to those in analogous macro scale systems, suggesting their use not only as nanoprinting devices but also as dynamic nanoscale reaction vessels.

A small number of pumping methodologies have been examined in the literature. Kral suggested setting up an electric current in the nanotube via laser excitation resulting in a net force on ions absorbed in the nanotube,[11] while Insepov et al., using molecular dynamics, demonstrate a method for activating axial gas flow inside a CNT by setting up Raleigh traveling waves on the nanotube surface.[12] Very recently Gong et al. used molecular dynamics to predict an induced directional flow in nanopores from the positioning of a combination of charges adjacent to the nanopores.[13] Here, using molecular dynamics (MD) and theoretical analysis, we describe a system whereby fluid, in this case decane, is imbibed from a reservoir at one end of the nanotube, heated, and subsequently effuses in a jet from the other end. The mechanism is related to the balance of pressures between a strongly imbibing fluid at room temperature and that of a dense hot supercritical fluid. We develop a simple kinetic theory analysis for the system that allows us to estimate the free energy barrier to effusion and predict pumping fluxes over a range of temperatures and nanotube diameters.

Our starting simulation cell comprises a [22,0] nanotube (1.72 nm diameter) 13.5 nm in length, aligned along the *z*-axis and immersed at one end in an essentially infinite slab of decane with imposed periodic boundary conditions in the *x* and *y* directions. A short-range repulsive wall stops decane from wetting the outer surface of the nanotube (Figure 1). The carbon potential was the reactive empirical bond order potential of Brenner,[14] while decane−decane and decane−carbon interactions were identical to those used in previous papers.[5] We would stress at this point that, while the decane potential model has been fitted to experimental data up to 650 K,[15] here we explore much higher temperature ranges, indeed temperatures and pressures at which thermal decomposition will occur.[16] The results here are intended to reflect qualitative behavior and should be seen as "proof of principle", but we also note that while we do not explicitly account for decomposition reactions, reactions will occur at these temperatures and pressures that are of interest in their own right and add weight to the idea that these devices can be considered nanoscale reaction vessels. While we have

* Author to whom correspondence should be addressed.

10.1021/nl071537e CCC: $37.00
Published on Web 10/13/2007

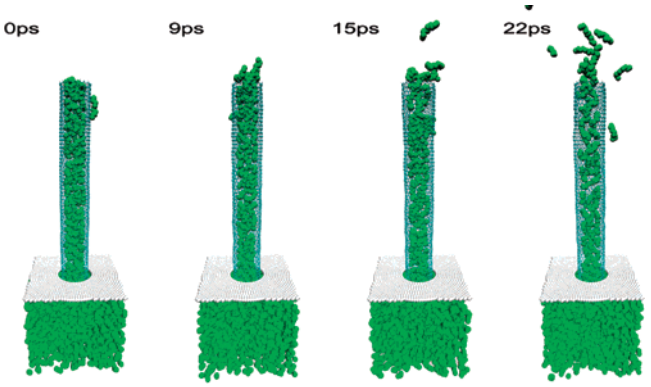

Figure 1. Snapshot of the simulation cell at intervals after the initialization of the heat source. A short-range repulsive wall (white) stops the fluid wetting the outside of the nanotube. Periodic boundary conditions are imposed in the directions perpendicular to the nanotube axis.

found it convenient to choose decane as the fluid, as we have much experience with the nanotube−decane system, we expect similar behavior with any fluid for which the nanotube−fluid surface tension suggests strong capillary imbibition.

Fluid is allowed to imbibe into the nanotube following the dynamics elucidated previously.[17,18] Two methods are explored for introducing heat into the system: stimulation of the radial breathing mode (RBM) of the CNT and thermostating the nanotube wall atoms to a particular temperature using a Berendsen[19] thermostat. The decane reservoir was maintained at a constant 300 K by an additional spatially restricted Berendsen thermostat. The RBM of CNTs is a Raman active mode that corresponds to the radially symmetrical "breathing-like" vibration of the carbon atoms. It is used extensively to characterize size distributions of nanotube samples, both in aqueous and nonaqueous environments, due to its inverse diameter proportionality. The RBM was simulated in the MD by adding an oscillating radial force field that acted only on the nanotube carbon atoms at the RBM frequency of the particular nanotube. The amplitude of the force field was used to control the strength of the RBM and hence the level of heat introduced into the system via direct collision of the nanotube walls with the adsorbed fluid. The system is shown in Figure 1 with snapshots at intervals from the initialization of the heat source.

Although it seems intuitive that the RBM method might act on the decane in a semimechanical way, essentially squeezing fluid along the nanotube much like in ref 12, actually the pumping dynamics of the system were defined entirely by the temperature of the fluid at the hot end of the nanotube, irrespective of the manner of heating. Further analysis of the trajectories revealed that even when the RBM raised the temperature of the fluid by 1000 K or more, the average variation in nanotube radius due to the RBM was only of the order of 0.1%, which is 1−2 orders of magnitude smaller than those in ref 12. Fluid temperature and density profiles along the nanotube axis (extending into the reservoir) are shown in Figure 2. The spatially restricted Berendsen thermostat acts to maintain the reservoir at 300 K, while inside the nanotube most of the heating of the imbibing fluid (transferred directly from the nanotube walls) occurs in the first third of the nanotube. The temperature and density of the fluid is fairly constant throughout the remaining two-thirds of the nanotube (dotted lines represent the two ends of the nanotube). The horizontal lines show the average axial temperature of the nanotube walls (whereby we consider contributions to the temperature from axial degrees of freedom only) to achieve this particular fluid temperature for both methods of heating. The lower (blue) line represents the RBM stimulation method, while the upper (red) line is the thermostat method. Note that for the RBM method, the fluid in the nanotube is hotter than the axial temperature of the nanotube walls, whereas for the thermostat method it is cooler. This is a consequence of the incomplete equipartition of energy; the external field introduces kinetic energy to the

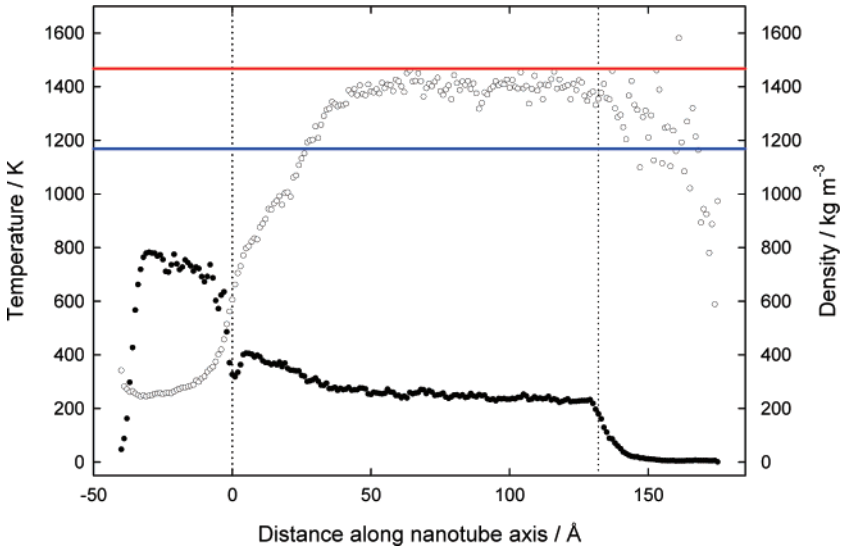

Figure 2. Fluid temperature (empty circles) and density (filled circles) profile along nanotube axis; nanotube ends are represented by dotted vertical lines. The horizontal lines represent the average axial temperature of the nanotube to achieve this fluid temperature under RBM stimulated heating (blue) and thermostat heating (red).

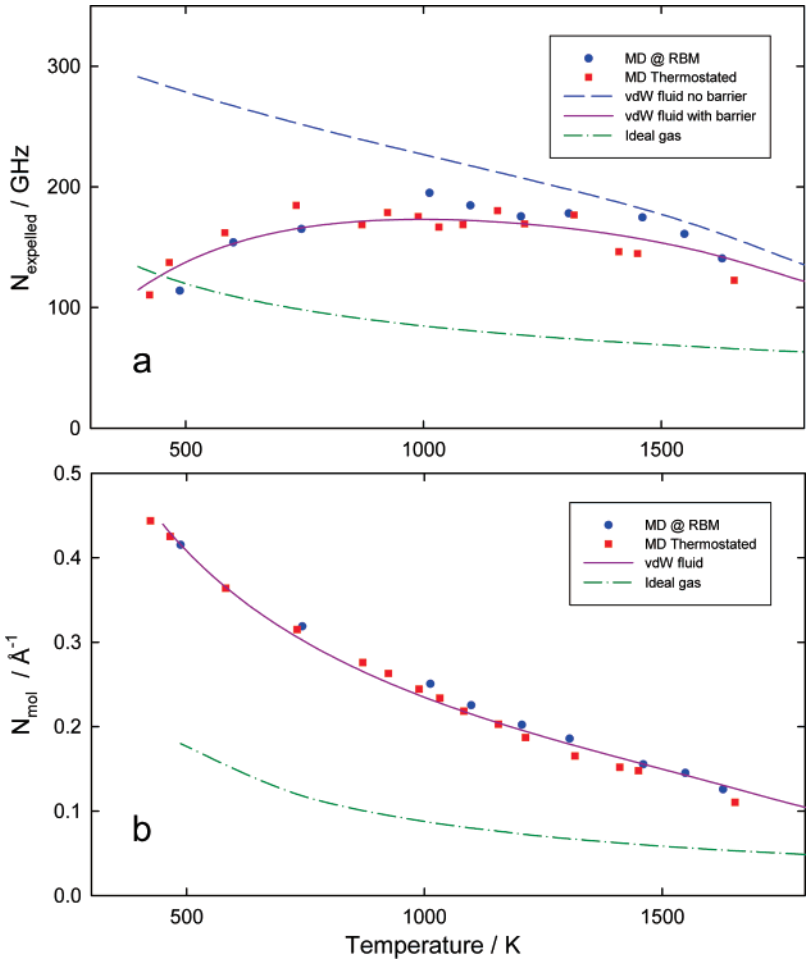

Figure 3. (a) Pumping flux as a function of tube-end fluid temperature. Points represent MD results for (blue circles) RBM stimulated heating and (red squares) thermostated heating. Lines represent analytical solutions for a van der Waal (vdW) fluid with no barrier to effusion (blue dashed), a vdW fluid with fitted free energy barrier to effusion (purple continuous), and an ideal gas (green dot dash). (b) The axial number density as a function of tube-end fluid temperature for RBM stimulated heating (blue circles) and thermostat heating (red squares). The data can be easily fitted to a vdW fluid with one temperature-dependent parameter $a(T)$ (purple line). The number density due to an ideal gas is shown for comparison (green dot dash).

radial modes of the nanotube of which a proportion is lost directly to the adsorbed fluid resulting in a lower temperature of the axial modes compared to the radial ones.

The pumping flux, defined as the number of molecules expelled from the nanotube per second, was monitored for the two methodologies over a range of tube-end fluid temperatures. The results can be seen in Figure 3a; the circular (blue) points represent the RBM stimulated method, and the square (red) points represent the thermostat method (errors bars are of the order of 20 GHz). There is no statistically important difference between the two methods of heating. This is further confirmed in Figure 3b, which plots the number density at the end of the nanotube as a function of tube-end fluid temperature. The pumping flux is a function of the tube-end fluid temperature and the tube-end number density, which in itself, is a function of the tube-end fluid temperature. Using kinetic theory as our starting point, we develop a simple analytical framework for the system.

We consider nanotubes to be one-dimensional systems, and consider only the axial z direction. Turning first to the hot end of the nanotube, the number of collisions per unit time with the end of the nanotube according to kinetic theory is

$$\rho A \int_0^\infty v_z f(v_z)\, \mathrm{d}v_z \tag{1}$$

where ρ is the tube-end fluid density, A is the accessible cross-sectional area of the nanotube (defined as the nanotube radius minus the Lennard-Jones radius of a carbon atom), v_z is the velocity of molecules in the axial direction and $f(v_z)$ is the Maxwell−Boltzmann velocity distribution in one dimension. If we impose a potential barrier V_B at the end of the nanotube, then only molecules with axial velocities greater than

$$v_{\min} = \sqrt{\frac{2V_B}{m}} \tag{2}$$

will escape the nanotube where m is the mass of the fluid molecules. The total number of collisions per unit time

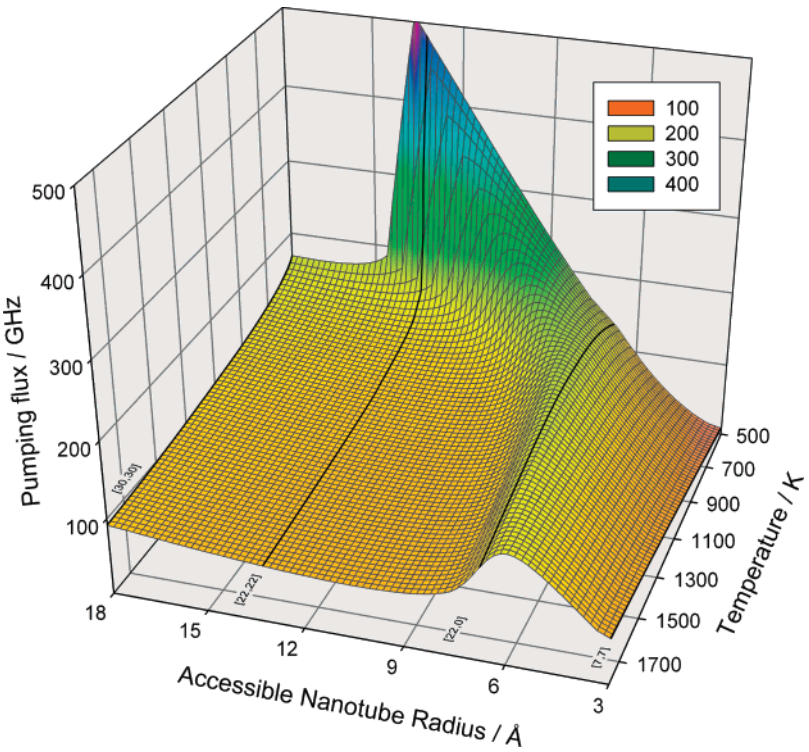

Figure 4. Pumping flux as a function of temperature and nanotube radius. Imbibing forces for the [7,7], [22,0], [22,22], and [30,30] nanotube are taken from our previous paper.[17]

resulting in a molecule being expelled from the nanotube is

$$\frac{N_{\text{expelled}}}{t} = \rho_z\left(\frac{m}{2\pi kT}\right)^{1/2} \int_{u_{\min}}^{\infty} e^{-u}\, du \tag{3}$$

where

$$u = \frac{m v_z^{\,2}}{2kT}, \qquad u_{\min} = \frac{V_B}{kT} \tag{4}$$

k is the Boltzmann constant, T is the tube-end fluid temperature, and ρ_z is the one-dimensional number density along the nanotube axis. This is easily solved and results in a pumping flux of

$$\frac{N_{\text{expelled}}}{t} = \rho_z\left(\frac{kT}{2\pi m}\right)^{1/2} e^{-V_B/kT} \tag{5}$$

The one-dimensional number density is also a function of tube-end fluid temperature and can be approximated in the following way. Once the system has reached a steady state, the pressure (upward) due to the imbibing fluid at the cold end of the nanotube must balance exactly the thermodynamic pressure (downward) at the hot end of the nanotube. The imbibing forces on the fluid at the reservoir end are related to the nanotube−fluid surface tensions and are given by

$$F_w = 2\Delta\gamma(r)\pi r \tag{6}$$

where we again define r as the accessible nanotube radius and $\Delta\gamma$ as the difference between the nanotube−fluid and the nanotube−vacuum/vapor surface tensions. Full details can be found in our previous papers on the dynamics of imbibition into carbon nanotubes.[17] The pressure in the fluid at the cold end of the nanotube is therefore given by

$$p_{\text{cold}} = \frac{2\Delta\gamma(r)}{r} \tag{7}$$

Values for $\Delta\gamma$ for different sized nanotubes are estimated in ref 17. As a simple approximation to an equation of state (EOS) for the decane, we assume a simple van der Waals form for the EOS

$$p_{\text{hot}} = \frac{NkT}{V - Nb} - a\rho^2 \tag{8}$$

where k is the Boltzmann constant, ρ is the density, V is the volume of the fluid, T is the temperature of the fluid, N is the number of molecules, b is the correction to the volume term, and a is the correction due to the attractive presence of the fluid. Following the standard approach, b is related to the critical temperature and pressure of decane[20]

$$b = \frac{RT_C}{8P_C} \tag{9}$$

whereas a is a temperature-dependent term that can be fitted

to reproduce the simulation data (Figure 3b). Expanding eq 8 in powers of ρ and equating it with eq 7 allows us to solve for the number density at a particular pressure and for a particular nanotube radius. The analytical results for the pumping flux are shown in Figure 3a as lines. The long dashed (blue) line represents the analytical pumping flux for the [22,0] nanotube assuming no barrier potential at the end of the nanotube, while the continuous purple line is with the addition of a barrier V_B, chosen so as to best match the simulation data. The height of this barrier can be interpreted as the free energy barrier to molecular effusion, and in the case of the [22,0] nanotube is of the order of 3 kJ mol^{-1}. This is surprisingly low when compared with the average adsorption energy of a decane molecule in the nanotube, which is about 60 kJ mol^{-1}, and results from the fact that the escape process for a molecule is rather more complicated than the simple model would suggest. Molecules do not simply effuse out of the end in a singular event but rather follow a series of processes that act to lower the energy barrier. These processes involve clustering of decane molecules, molecules "dragging" other molecules out, and increased mechanical pressures due to the flexing H-terminated nanotube ends. While these processes are interesting in their own right, for the present study we may consider the effusion event, described by eq 3, as the trigger for a series of processes leading, on average, to a molecule escaping from the nanotube.

Figure 4 plots the pumping flux as a function of temperature and accessible nanotube radius between 3 and 18 Å, corresponding to a [7,7] and a [30,30] nanotube (nanotubes for which the imbibing forces are known). The "radius" axis can also be thought of as the pressure in the nanotube as a result of imbibition and ranges from about 63 MPa for the [7,7] nanotube to about 1 MPa for the [30,30] nanotube (though it does not vary linearly with radius; see ref 17 for details). For small nanotube radii, the pumping flux is almost zero at low temperatures, rising only to about 50 GHz at 1600 K. The low flux is due both to the low axial number density (typically single file decane) as well as the relatively high free-energy barrier ($\sim$10 kJ mol^{-1}) compared to the larger nanotubes. As we increase in radius toward the [22,0] nanotube, there is a region of elevated flux over the whole temperature range. This is caused by high imbibition pressures (8 MPa) in the nanotube maintaining a dense supercritical fluid throughout the temperature range. As temperatures increase, the decrease in fluid density offsets the increased probability of effusion upon tube-end collisions. As we approach the [22,22] nanotube, a large peak is seen in the low-temperature region. This reflects the discontinuity in density caused by the liquid−gas phase transition that occurs below the critical pressure of about 2 MPa. At higher temperatures, the density of the gas and hence the pumping flux is low. As we further increase nanotube radius, the phase transition moves to lower temperatures, tending toward the atmospheric pressure value of 447 K. Increasing nanotube radii yet further, we see reduced imbibing pressures and free-energy barriers; much of the interesting behavior disappears and we simply have directed evaporation with an ever increasing nozzle size.

Although, as we have mentioned, these results should be treated as qualitative due to our use of potentials beyond their "testing ground", the ideas presented are simple and intuitive, and the proof of principle for possible applications is clear. Where capillary forces act to draw molecules into nanopores, heating and effusion will act to expel them. In fact, similar principles have formed the basis of ink-jet technology since the 1970s. What is extraordinary at the nanoscale, however, is the magnitude of the pressures that build up inside these miniature vessels, opening up the possibility not only of nanoscale printing, but also of continuous jet nanoscale reactors. The desire to process minute quantities of fluids along with the interest in high throughput systems is increasing rapidly; a system, such as the one described in this letter, might serve as a valuable addition to the ever extending lab-on-a-chip toolbox.

References

(1) Iijima, S. *Nature* **1991**, *354* (6348), 56.
(2) Whitby, M.; Quirke, N. *Nat Nanotechnol.* **2007**, *2* (2), 87.
(3) Holt, J. K.; Park, H. G.; Wang, Y. M.; Stadermann, M.; Artyukhin, A. B.; Grigoropoulos, C. P.; Noy, A.; Bakajin, O. *Science* **2006**, *312* (5776), 1034.
(4) Sriraman, S.; Kevrekidis, I. G.; Hummer, G. *Phys. Rev. Lett.* **2005**, *95* (13), 130603.
(5) Supple, S.; Quirke, N. *Phys. Rev. Lett.* **2003**, *90* (21), 214501.
(6) Longhurst, M. J.; Quirke, N. *Phys. Rev. Lett.* **2007**, *98*, 145503.
(7) Wang, J. *Electroanalysis* **2005**, *17* (1), 7.
(8) Pagona, G.; Tagmatarchis, N. *Curr. Med. Chem.* **2006**, *13* (15), 1789.
(9) Dai, H. **2002**, *35*, 1035.
(10) Pan, X.; Fan, Z.; Chen, W.; Ding, Y.; Luo, H.; Bao, X. *Nat. Mater.* [Online early access] (2007).
(11) Kral, P.; Tomanek, D. *Phys. Rev. Lett.* **1999**, *82* (26), 5373.
(12) Insepov, Z.; Wolf, D.; Hassanein, A. *Nano Letters* **2006**, *6* (9), 1893.
(13) Gong, X.; Li, J.; Lu, H.; Wan, R.; Li, J.; Hu, J.; Fang, H. *Nat. Nanotechnol.*, in press.
(14) Brenner, D. W.; Shenderova, O. A.; Harrison, J. A.; Stuart, S. J.; Ni, B.; Sinnott, S. B. *J. Phys:.Condens. Matter* **2002**, *14* (4), 783.
(15) Supple, S.; Quirke, N. *Mol. Simul.* **2003**, *29* (2), 77.
(16) Stubbs, F. J.; Hinshelwood, C. *Proc. R. Soc., London, Sect. A* **1950**, *200* (1063), 458.
(17) Supple, S.; Quirke, N. *J. Chem. Phys.* **2004**, *121* (17), 8571.
(18) Supple, S.; Quirke, N. *J. Chem. Phys.* **2005**, *122* (10), 104706.
(19) Berendsen, H. J. C.; Postma, J. P. M.; Vangunsteren, W. F.; Dinola, A.; Haak, J. R. *J. Chem. Phys.* **1984**, *81* (8), 3684.
(20) Timmermans, J. *Physico-Chemical Constants of Pure Organic Compounds*; Elsevier: New York, 1950.

NL071537E